

$B_s \rightarrow K^{(*)-} K^{(*)+}, K^{(*)-} \pi^+, K^{(*)-} \rho^+$ decays in R-parity violating supersymmetry

Yuan-Guo Xu^{1,2}, Ru-Min Wang³ and Ya-Dong Yang^{1,2} *

¹*Key Laboratory of Quark & Lepton Physics (Huazhong Normal University),*

Ministry of Education, P.R. China

²*Institute of Particle Physics, Huazhong Normal University, Wuhan, Hubei 430079, P.R.China* [†]

³*Department of Physics, Yonsei University, Seoul 120-479, Korea*

June 6, 2022

Abstract

With the first measurements of the branching ratios and the direct CP asymmetries of $B_s \rightarrow K^- K^+, K^- \pi^+$ decays by the CDF collaboration, we constrain the relevant parameter space of the Minimal Supersymmetric Standard Model with R-parity violation. Using the constrained R-parity violating couplings, we further examine their possible effects in $B_s \rightarrow K^{*-} \pi^+, K^{(*)-} \rho^+$ and $K^{(*)\pm} K^{(*)\mp}$ decays. We find that some branching ratios and CP asymmetries are very sensitive to the R-parity violating couplings. The direct longitudinal CP asymmetries of tree-dominated process $B_s \rightarrow K^{*-} \rho^+$ could be enlarged to $\sim 70\%$ and the longitudinal polarizations of $B_s \rightarrow K^{*-} K^{*+}, K^{*-} \rho^+$ decays could be suppressed very much by the squark exchange couplings. Near future experiments at CERN LHC can test these predictions and shrink/reveal the parameter spaces of RPV SUSY.

PACS Numbers: 12.60.Jv, 12.15.Ji, 12.38.Bx, 13.25.Hw

*Corresponding author, yangyd@iopp.ccnu.edu.cn

[†]Mailing address

1 Introduction

In the recent ten years, the successful running of B factories BABAR and Belle has provided rich experimental data for B^\pm and B^0 , which has confirmed the Kobayashi-Maskawa CP asymmetry mechanism in the Standard Model (SM) and also shown hints for new physics (NP). Among the rich phenomena of B decays, the two-body charmless decays are the known effective probes of the CP violation in the SM and are sensitive to potential NP scenarios beyond the SM. The two body charmless B_s decays will play the same important role for studying the CP asymmetries (CPA), determining CKM matrix elements and constraining/seraching for the indirect effects of various NP scenarios.

Recently the CDF collaboration at Fermilab Tevatron has made the first measurement of charmless two-body B_s decays [1, 2, 3, 4, 5]

$$\begin{aligned}\mathcal{B}(B_s \rightarrow K^- K^+) &= (24.4 \pm 1.4 \pm 3.5) \times 10^{-6}, \\ \mathcal{B}(B_s \rightarrow K^- \pi^+) &= (5.0 \pm 0.7 \pm 0.8) \times 10^{-6}, \\ \mathcal{A}_{CP}^{dir}(B_s \rightarrow K^- \pi^+) &= 0.39 \pm 0.15 \pm 0.08.\end{aligned}\tag{1}$$

The measurement is an important mark of B_s physics, and also implies that many B_s decay modes could be precisely measured at the coming LHCb.

Compared with the theoretical predictions for these quantities in Refs. [6], [7] and [8], based on the QCD factorization approach (QCDF) [9], the perturbative QCD (PQCD) [10], and the soft-collinear effective theory (SCET) [11], respectively, one would find the experimental measurements of branching ratios agree with the SM predictions within their large theoretical uncertainties. However, NP effects would be still possible to render other observable deviated from the SM expectation with the branching ratios nearly unaltered [12].

The related decays $B_s \rightarrow K^{(*)-} K^{(*)+}$, $K^{(*)-} \pi^+$, $K^{(*)-} \rho^+$ have also been extensively studied in the literature [6, 7, 8, 13, 14, 15]. The four decays $B_s \rightarrow K^{(*)-} K^{(*)+}$ are governed by the $\bar{b} \rightarrow \bar{s} u \bar{u}$ transition at the quark level, which are penguin-dominated processes. The tree-dominated decays $B_s \rightarrow K^{(*)-} \pi^+$, $K^{(*)-} \rho^+$ are induced by $\bar{b} \rightarrow \bar{u} u \bar{d}$ where the direct CPA are expected to be small in the SM. At present, among many measurements of $B_{u,d}$ decays, several discrepancies with the SM predictions have appeared in the corresponding penguin-dominated $\bar{b} \rightarrow \bar{s} q \bar{q}$ ($q = u, d, s$) processes and tree-dominated $\bar{b} \rightarrow \bar{d} q' \bar{q}'$ ($q' = u, d$) processes. For example,

$B \rightarrow \pi\pi, \pi K$ puzzles [16, 17, 18, 19, 20] and the large transverse polarization anomaly in $B \rightarrow \rho K^*, \phi K^*$ decays [21, 22, 23]. Although the discrepancies are not statistically significant, there is an unifying similarity pointing to NP (for example, [12, 24, 25, 26, 27, 28, 29, 30]). There could be also potential NP contributions in $B_s \rightarrow K^{(*)-} K^{(*)+}, K^{(*)-} \pi^+, K^{(*)-} \rho^+$ decays, which have been analyzed with different NP models [12, 30, 31, 32]. The measurements given in Eq. (1) will afford an opportunity to constrain NP scenarios beyond the SM.

Among the NP models that survived electroweak data, one of the respectable options is the R-parity violating (RPV) supersymmetry (SUSY). The possible appearance of the RPV couplings [33, 34], which will violate the lepton and baryon number conservation, has gained full attentions in searching for SUSY [35, 36, 37, 38]. In this work, we will study the $B_s \rightarrow K^{(*)-} K^{(*)+}, K^{(*)-} \pi^+$ and $K^{(*)-} \rho^+$ decays in the Minimal Supersymmetric Standard Model (MSSM) with R-parity violation by employing the QCDF. The four $B_s \rightarrow K^{(*)+} K^{(*)-}$ decays are all induced at the quark level by $\bar{b} \rightarrow \bar{s} u \bar{u}$ process, they involve the same set of RPV coupling constants. The $B_s \rightarrow K^{(*)-} \pi^+, K^{(*)-} \rho^+$ decays are due to $\bar{b} \rightarrow \bar{d} u \bar{u}$ at the quark level, and they also involve the same set of RPV coupling constants. Using the latest experimental data and the theoretical parameters, we have derived new bounds on the relevant R-parity violating couplings, which are consistent with the bounds from $B_{u,d}$ decays. With the constrained parameter spaces, we predict the RPV effects on the other quantities in $B_s \rightarrow K^{(*)-} K^{(*)+}, K^{(*)-} \pi^+$ and $K^{(*)-} \rho^+$ decays which have not been measured yet. We find that the R-parity violating effects on some branching ratios and direct CPA could be large. For example, the squark exchange couplings could enhance the direct CP asymmetry in the longitudinal polarized mode of $B_s \rightarrow K^{*-} \rho^+$ to $\sim 73\%$ and suppress the longitudinal polarization fractions of $B_s \rightarrow K^{*-} K^{*+}$ and $K^{*-} \rho^+$ to ~ 0.5 . The mixing-induced CPA are also found to be sensitive to the RPV effects. Therefore, with the ongoing B-physics at Tevatron, in particular with the onset of the LHC-b experiment, we expect a wealth of B_s decays data and measurements of these observables could restrict or reveal the NP parameter spaces in the near future.

The paper is arranged as follows. In Sec. 2, we give the expression of the CP averaged branching ratios, the direct CPA, the mixing-induced CPA and the polarization fractions within the QCDF approach in $B_s \rightarrow K^{(*)-} K^{(*)+}, K^{(*)-} \pi^+, K^{(*)-} \rho^+$ systems, where the RPV SUSY effects are included. We also tabulate the theoretical inputs in this section. Sec. 3 deals with

the numerical results. We display the constrained parameter spaces which satisfy the present experimental data of B_s decays, and then we use the constrained parameter spaces to predict the RPV effects on the other observable quantities, which have not been measured yet in $B_s \rightarrow K^{(*)-} K^{(*)+}$, $K^{(*)-} \pi^+$ and $K^{(*)-} \rho^+$ decays. Sec. 4 contains our summary and conclusion.

2 The theoretical frame for $B \rightarrow M_1 M_2$ decays

2.1 The decay amplitudes in the SM

In the SM, the low energy effective Hamiltonian for the $\Delta B = 1$ transition at the scale $\mu \sim m_b$ is given by [39]

$$\mathcal{H}_{eff}^{SM} = \frac{G_F}{\sqrt{2}} \sum_{p=u,c} \lambda_p^q \left(C_1 Q_1^p + C_2 Q_2^p + \sum_{i=3}^{10} C_i Q_i + C_{7\gamma} Q_{7\gamma} + C_{8g} Q_{8g} \right) + \text{h.c.}, \quad (2)$$

here $\lambda_p^q = V_{pb} V_{pq}^*$ for $b \rightarrow q$ transition ($p \in \{u, c\}, q \in \{d, s\}$) and the detailed definition of the operator base can be found in [39].

With the weak effective Hamiltonian given by Eq. (2), one can write the decay amplitudes for the general two-body hadronic $B \rightarrow M_1 M_2$ decays as

$$\begin{aligned} \mathcal{A}^{SM}(B \rightarrow M_1 M_2) &= \langle M_1 M_2 | \mathcal{H}_{eff}^{SM} | B \rangle \\ &= \sum_p \sum_i \lambda_p^q C_i(\mu) \langle M_1 M_2 | Q_i(\mu) | B \rangle. \end{aligned} \quad (3)$$

The essential theoretical difficulty for obtaining the decay amplitude arises from the evaluation of hadronic matrix elements $\langle M_1 M_2 | Q_i(\mu) | B \rangle$, for which we will employ the QCDF [9] throughout this paper.

The QCDF [9] allows us to compute the non-factorizable corrections to the hadronic matrix elements $\langle M_1 M_2 | Q_i | B \rangle$ in the heavy quark limit. The factorization formula reads

$$\langle M_1 M_2 | Q_i | B \rangle = \left(F_j^{B \rightarrow M_1} T_{ij}^I * f_{M_2} \Phi_{M_2} + [M_1 \leftrightarrow M_2] \right) + T_i^{II} * f_B \Phi_B * f_{M_1} \Phi_{M_1} * f_{M_2} \Phi_{M_2}, \quad (4)$$

where $F_j^{B \rightarrow M_1}$ is the appropriate form factor, Φ_M are leading-twist light-cone distribution amplitudes and the star products imply an integration over light-cone momentum fractions. By the above factorization formula, the complicated hadronic matrix elements of four-quark operators are reduced to simpler non-perturbative quantities and calculable hard-scattering kernels $T^{I,II}$.

Then the decay amplitude has the form

$$\mathcal{A}^{SM}(B \rightarrow M_1 M_2) = \sum_p \sum_i \lambda_p^q \left\{ a_i^p \langle M_2 | J_2 | 0 \rangle \langle M_1 | J_1 | B \rangle + b_i^p \langle M_1 M_2 | J_2 | 0 \rangle \langle 0 | J_1 | B \rangle \right\}, \quad (5)$$

where the effective parameters a_i^p including nonfactorizable corrections at order of α_s . They are calculated from the vertex corrections, the hard spectator scattering, and the QCD penguin contributions. The parameters b_i^p are calculated from the weak annihilation contributions. The factorized matrix element is given by

$$A_{M_1 M_2} \equiv \langle M_2 | (\bar{q}_2 \gamma_\mu (1 - \gamma_5) q_3) | 0 \rangle \langle M_1 | (\bar{b} \gamma^\mu (1 - \gamma_5) q_1) | B \rangle, \quad (6)$$

which can be expressed in terms of the corresponding decay constants and form factors. We will use the QCDF amplitudes of these decays derived in the comprehensive papers [6, 13] as inputs for the SM amplitudes.

2.2 R-parity violating SUSY effects in the decays

In the most general superpotential of MSSM, the RPV superpotential is given by [33]

$$\mathcal{W}_{RPV} = \mu_i \hat{L}_i \hat{H}_u + \frac{1}{2} \lambda_{[ij]k} \hat{L}_i \hat{L}_j \hat{E}_k^c + \lambda'_{ijk} \hat{L}_i \hat{Q}_j \hat{D}_k^c + \frac{1}{2} \lambda''_{i[jk]} \hat{U}_i^c \hat{D}_j^c \hat{D}_k^c, \quad (7)$$

where \hat{L} and \hat{Q} are the SU(2)-doublet lepton and quark superfields and \hat{E}^c , \hat{U}^c and \hat{D}^c are the singlet superfields, while i , j and k are generation indices and c denotes a charge conjugate field.

The bilinear RPV superpotential terms $\mu_i \hat{L}_i \hat{H}_u$ can be rotated away by suitable redefining the lepton and Higgs superfields [35]. However, the rotation will generate a soft SUSY breaking bilinear term which would affect our calculation through penguin level. However, the processes discussed in this paper could be induced by tree-level RPV couplings, so that we would neglect sub-leading RPV penguin contributions in this study.

The λ and λ' couplings in Eq. (7) break the lepton number, while the λ'' couplings break the baryon number. There are 27 λ'_{ijk} couplings, 9 λ_{ijk} and 9 $\lambda''_{i[jk]}$ couplings. $\lambda_{[ij]k}$ are antisymmetric with respect to their first two indices, and $\lambda''_{i[jk]}$ are antisymmetric with j and k .

From Eq. (7), we can obtain the relevant RPV effective Hamiltonian as shown in Fig. 1

$$\mathcal{H}_{eff}^{RPV} = \sum_i \frac{\lambda'_{ijm} \lambda_{ikl}^*}{2m_{\tilde{e}_{Li}}^2} \eta^{-8/\beta_0} (\bar{d}_m \gamma^\mu P_R d_l)_8 (\bar{u}_k \gamma_\mu P_L u_j)_8$$

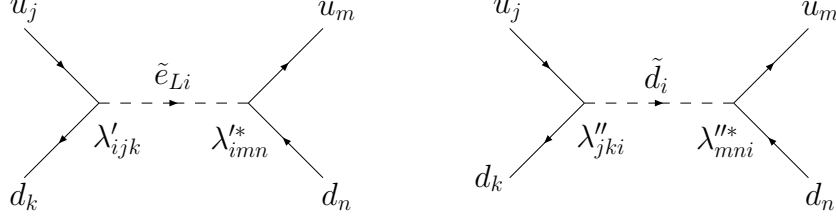


Figure 1: RPV tree level contributions to $b \rightarrow u\bar{u}q$ process.

$$\begin{aligned}
& + \sum_n \frac{\lambda''_{ikn} \lambda''^*_{jln}}{2m_{\tilde{d}_n}^2} \eta^{-4/\beta_0} \left\{ [(\bar{u}_i \gamma^\mu P_R u_j)_1 (\bar{d}_k \gamma_\mu P_R d_l)_1 - (\bar{u}_i \gamma^\mu P_R u_j)_8 (\bar{d}_k \gamma_\mu P_R d_l)_8] \right. \\
& \left. - [(\bar{d}_k \gamma^\mu P_R u_j)_1 (\bar{u}_i \gamma_\mu P_R d_l)_1 - (\bar{d}_k \gamma^\mu P_R u_j)_8 (\bar{u}_i \gamma_\mu P_R d_l)_8] \right\}, \quad (8)
\end{aligned}$$

where Eq. (8), $P_L = \frac{1-\gamma_5}{2}$, $P_R = \frac{1+\gamma_5}{2}$, $\eta = \frac{\alpha_s(m_{\tilde{f}})}{\alpha_s(m_b)}$ and $\beta_0 = 11 - \frac{2}{3}n_f$. The subscript of the currents $(j_\mu)_{1,8}$ represents the current in the color singlet and octet, respectively. The coefficients η^{-4/β_0} and η^{-8/β_0} are due to the running from the sfermion mass scale $m_{\tilde{f}}$ (100 GeV assumed) down to the m_b scale. Since it is always assumed in phenomenology numerical display that only one sfermion contributes at one time, we neglect the mixing between the operators when we use the renormalization group equation to run \mathcal{H}_{eff}^{RPV} down to the low scale.

The RPV amplitude for the decays can be written as

$$\mathcal{A}^{RPV}(B \rightarrow M_1 M_2) = \langle M_1 M_2 | \mathcal{H}_{eff}^{RPV} | B \rangle. \quad (9)$$

Generally, the product RPV couplings can be complex and their phases may induce new contribution to CP violation, which we write as

$$\Lambda_{ijk} \Lambda_{lmn}^* = |\Lambda_{ijk} \Lambda_{lmn}| e^{i\phi_{RPV}}, \quad \Lambda_{ijk}^* \Lambda_{lmn} = |\Lambda_{ijk} \Lambda_{lmn}| e^{-i\phi_{RPV}}. \quad (10)$$

The RPV coupling constant $\Lambda \in \{\lambda, \lambda', \lambda''\}$, and ϕ_{RPV} is the RPV weak phase, which may take any value between $-\pi$ and π .

For simplicity we only consider the vertex corrections and the hard spectator scattering in the RPV decay amplitudes. We ignore the RPV penguin contributions, which are expected to be small even compared to the SM penguin amplitudes, this follows from the smallness of the relevant RPV couplings compared to the SM gauge couplings. Thus, the bounds on the RPV couplings are insensitive to the inclusion of the RPV penguins [40]. We also neglected the annihilation contributions in the RPV amplitudes. After Fierz transformations, the relevant NP operators due to squark exchanges are $(\bar{u}\gamma_\mu(1+\gamma_5)q)(\bar{b}\gamma^\mu(1+\gamma_5)u)$ and $(\bar{u}\gamma_\mu(1-\gamma_5)u)(\bar{b}\gamma^\mu(1+$

$\gamma_5)q)$. The factorized matrix element of these new RPV operators is given as follows

$$A'_{M_1 M_2} \equiv \langle M_2 | (\bar{u} \gamma_\mu (1 + \gamma_5) q) | 0 \rangle \langle M_1 | (\bar{b} \gamma^\mu (1 + \gamma_5) u) | B \rangle, \quad (11)$$

$$= -i \begin{cases} m_B^2 f_{M_2} F_0^{B \rightarrow M_1}(0), & \text{if } M_1 = M_2 = P, \\ m_B^2 f_{M_2} A_0^{B \rightarrow M_1}(0), & \text{if } M_1 = V, M_2 = P, \\ m_B^2 f_{M_2} F_+^{B \rightarrow M_1}(0), & \text{if } M_1 = P, M_2 = V, \\ m_B^2 f_{M_2} A_0^{B \rightarrow M_1}(0), & \text{if } M_1 = M_2 = V \text{ and } h = 0, \\ m_B m_{M_2} f_{M_2} F_{\mp}^{B \rightarrow V_1}(0), & \text{if } M_1 = M_2 = V \text{ and } h = \pm, \end{cases} \quad (12)$$

with

$$F_{\pm}^{B \rightarrow V_1}(q^2) \equiv \left(1 + \frac{m_{V_1}}{m_B}\right) A_1^{B \rightarrow V_1}(q^2) \mp \left(1 - \frac{m_{V_1}}{m_B}\right) V^{B \rightarrow V_1}(q^2). \quad (13)$$

Using QCDF, we can obtain the RPV amplitudes of $B_s \rightarrow K^{(*)-} K^{(*)+}$, $K^{(*)-} \pi^+$, $K^{(*)-} \rho^+$ decays. There are two independent RPV amplitudes, given by

$$\mathcal{A}^{RPV}(\bar{B}_s \rightarrow K^+ K^-) = -\frac{\lambda_{131}'' \lambda_{121}''}{8m_d^2} \eta^{-4/\beta_0} F_{K\bar{K}} A'_{K\bar{K}} - \frac{\lambda_{i13}^* \lambda_{i12}'}{8m_{\bar{e}_{Li}}^2} \eta^{-8/\beta_0} r_\chi^{K^+} N'(K) A'_{K\bar{K}}, \quad (14)$$

$$\mathcal{A}^{RPV}(\bar{B}_s \rightarrow K^+ \pi^-) = -\frac{\lambda_{132}'' \lambda_{112}''}{8m_s^2} \eta^{-4/\beta_0} F_{K\pi} A'_{K\pi} - \frac{\lambda_{i13}^* \lambda_{i11}'}{8m_{\bar{e}_{Li}}^2} \eta^{-8/\beta_0} r_\chi^{\pi^+} N'(\pi) A'_{K\pi}. \quad (15)$$

with $N'(M_2) = 1$ if $M_2 = P$ and $N'(M_2) = 0$ if $M_2 = V$. $F_{M_1 M_2}$ is defined as

$$F_{M_1 M_2} \equiv 1 - \frac{1}{N_c} + \frac{\alpha_s}{4\pi} \frac{C_F}{N_c} \left[V'(M_2) + \frac{4\pi^2}{N_c} H'(M_1 M_2) \right], \quad (16)$$

where $V'(M_2)$ and $H'(M_1 M_2)$ are the one-loop vertex corrections and hard spectator interactions for the new RPV operators, respectively. The RPV amplitudes for $\bar{B}_s \rightarrow K^+ K^{*-}$, $\bar{B}_s \rightarrow K^{*+} K^-$ and $\bar{B}_s \rightarrow K^{*+} K^{*-}$ are obtained from Eq. (14) by replacing $(K\bar{K}) \rightarrow (K\bar{K}^*)$, $(K\bar{K}) \rightarrow (K^* \bar{K})$ and $(K\bar{K}) \rightarrow (K^* \bar{K}^*)$, respectively. The RPV amplitudes for $\bar{B}_s \rightarrow K^+ \rho^{*-}$, $\bar{B}_s \rightarrow K^{*+} \pi^-$ and $\bar{B}_s \rightarrow K^{*+} \rho^{*-}$ are obtained from Eq. (15) by replacing $(K\pi) \rightarrow (K\rho^*)$, $(K\pi) \rightarrow (K^* \pi)$ and $(K\pi) \rightarrow (K^* \rho)$, respectively.

As for $V'(M_2)$ and $H'(M_1 M_2)$ for $M_1 M_2 = PP, PV, VP, VV$ cases, the explicit results are same as these of SM operator $(\bar{u} \gamma_\mu (1 - \gamma_5) q)(\bar{b} \gamma^\mu (1 - \gamma_5) u)$ except ones for $B \rightarrow VV$ and $h = \pm$ case. And we get

$$V'^-(V) = 0, \quad V'^+(V) = V^-(V). \quad (17)$$

$$H'^-(VV) = 0, \quad H'^+(VV) = -H^-(VV). \quad (18)$$

2.3 The total decay amplitude

From the above discussions, the total decay amplitude are then given as

$$\mathcal{A}(B_s \rightarrow M_1 M_2) = \mathcal{A}^{SM}(B_s \rightarrow M_1 M_2) + \mathcal{A}^{RPV}(B_s \rightarrow M_1 M_2). \quad (19)$$

The corresponding branching ratios read

$$\mathcal{B}(B_s \rightarrow M_1 M_2) = \frac{\tau_{B_s} |p_c|}{8\pi m_{B_s}^2} |\mathcal{A}(B_s \rightarrow M_1 M_2)|^2, \quad (20)$$

where τ_{B_s} is the B_s lifetime, $|p_c|$ is the center of mass momentum in the center of mass frame of the B_s meson. In the $B \rightarrow VV$ decay, the two vector mesons have the same helicity, therefore three different polarization states are possible, one longitudinal and two transverse, and we define the corresponding amplitudes as $\mathcal{A}_{0,\pm}$. Transverse ($\mathcal{A}_{\parallel,\perp}$) and helicity (\mathcal{A}_{\pm}) amplitudes are related by $\mathcal{A}_{\parallel,\perp} = \frac{\mathcal{A}_+ \pm \mathcal{A}_-}{\sqrt{2}}$. Then we have

$$|\mathcal{A}(B \rightarrow VV)|^2 = |\mathcal{A}_0|^2 + |\mathcal{A}_+|^2 + |\mathcal{A}_-|^2 = |\mathcal{A}_0|^2 + |\mathcal{A}_{\parallel}|^2 + |\mathcal{A}_{\perp}|^2. \quad (21)$$

The longitudinal polarization fraction f_L is defined by

$$f_L(B \rightarrow VV) = \frac{\Gamma_L}{\Gamma} = \frac{|\mathcal{A}_0|^2}{|\mathcal{A}_0|^2 + |\mathcal{A}_{\parallel}|^2 + |\mathcal{A}_{\perp}|^2}. \quad (22)$$

For the CPA of neutral B meson decays, there is an additional complication due to $B^0 - \bar{B}^0$ mixing. There are four cases that one encounters for neutral B^0 decays, as discussed in Ref. [41, 42, 43, 44].

- **Case (i):** $B^0 \rightarrow f, \bar{B}^0 \rightarrow \bar{f}$, where f or \bar{f} is not a common final state of B^0 and \bar{B}^0 , for example $B_s^0 \rightarrow K^- \pi^+, K^- \rho^+, K^{*-} \pi^+, K^{*-} \rho^+$.
- **Case (ii):** $B^0 \rightarrow (f = \bar{f}) \leftarrow \bar{B}^0$ with $f^{CP} = \pm f$, involving final states which are CP eigenstates, i.e., decays such as $B_s^0 \rightarrow K^- K^+$.
- **Case (iii):** $B^0 \rightarrow (f = \bar{f}) \leftarrow \bar{B}^0$ with $f^{CP} \neq \pm f$, involving final states which are not CP eigenstates. They include decays such as $B^0 \rightarrow (VV)^0$, as the VV states are not CP eigenstates.
- **Case (iv):** $B^0 \rightarrow (f \& \bar{f}) \leftarrow \bar{B}^0$ with $f^{CP} \neq f$, i.e., both f and \bar{f} are common final states of B^0 and \bar{B}^0 , but they are not CP eigenstates. Decays $B_s^0(\bar{B}_s^0) \rightarrow K^{*-} K^+, K^- K^{*+}$ belong to this case.

For CP case (i) decays, there is only direct CPA \mathcal{A}_{CP}^{dir} since no mixing is involved for these decays. For cases (ii) and (iii), their CPA would involve $B^0 - \bar{B}^0$ mixing. The direct CPA \mathcal{A}_{CP}^{dir} and the mixing-induced CPA \mathcal{A}_{CP}^{mix} are defined as¹

$$\mathcal{A}_{CP}^{k,dir}(B^0 \rightarrow f) = \frac{|\lambda_k|^2 - 1}{|\lambda_k|^2 + 1}, \quad \mathcal{A}_{CP}^{k,mix}(B^0 \rightarrow f) = \frac{2\text{Im}(\lambda_k)}{|\lambda_k|^2 + 1}, \quad (23)$$

where $k = 0, \parallel, \perp$ for $B \rightarrow VV$ decays and $k = 0$ for $B \rightarrow PP, PV$ decays, in addition, $\lambda_k = \frac{q}{p} \frac{\mathcal{A}_k(\bar{B}^0 \rightarrow \bar{f})}{\mathcal{A}_k(B^0 \rightarrow f)}$ for CP case (i) and $\lambda_k = \frac{q}{p} \frac{\mathcal{A}_k(\bar{B}^0 \rightarrow f)}{\mathcal{A}_k(B^0 \rightarrow f)}$ for CP cases (ii) and (iii).

Case (iv) also involves mixing but requires additional formulas. Here one needs the four time-dependent decay widths for $B^0(t) \rightarrow f$, $\bar{B}^0(t) \rightarrow \bar{f}$, $B^0(t) \rightarrow \bar{f}$ and $\bar{B}^0(t) \rightarrow f$ [41, 42, 43, 44]. These time-dependent widths can be expressed by four basic matrix elements [44]

$$\begin{aligned} g &= \langle f | \mathcal{H}_{eff} | B^0 \rangle, & h &= \langle f | \mathcal{H}_{eff} | \bar{B}^0 \rangle, \\ \bar{g} &= \langle \bar{f} | \mathcal{H}_{eff} | \bar{B}^0 \rangle, & \bar{h} &= \langle \bar{f} | \mathcal{H}_{eff} | B^0 \rangle, \end{aligned} \quad (24)$$

which determine the decay matrix elements of $B^0 \rightarrow f \& \bar{f}$ and $\bar{B}^0 \rightarrow f \& \bar{f}$ at $t = 0$. We will also study the following quantities

$$\mathcal{A}_{CP}^{k,dir}(B^0 \& \bar{B}^0 \rightarrow f) = \frac{|\lambda'_k|^2 - 1}{|\lambda'_k|^2 + 1}, \quad \mathcal{A}_{CP}^{k,mix}(B^0 \& \bar{B}^0 \rightarrow f) = \frac{2\text{Im}(\lambda'_k)}{|\lambda'_k|^2 + 1}, \quad (25)$$

$$\mathcal{A}_{CP}^{k,dir}(B^0 \& \bar{B}^0 \rightarrow \bar{f}) = \frac{|\lambda''_k|^2 - 1}{|\lambda''_k|^2 + 1}, \quad \mathcal{A}_{CP}^{k,mix}(B^0 \& \bar{B}^0 \rightarrow \bar{f}) = \frac{2\text{Im}(\lambda''_k)}{|\lambda''_k|^2 + 1}, \quad (26)$$

with $\lambda'_k = \frac{q}{p}(h/g)$ and $\lambda''_k = \frac{q}{p}(\bar{g}/\bar{h})$. The signature of CP violation is $\Gamma(\bar{B}^0(t) \rightarrow \bar{f}) \neq \Gamma(B^0(t) \rightarrow f)$ and $\Gamma(\bar{B}^0(t) \rightarrow f) \neq \Gamma(B^0(t) \rightarrow \bar{f})$, which means that $\mathcal{A}_{CP}^{k,dir}(B^0 \& \bar{B}^0 \rightarrow f) \neq -\mathcal{A}_{CP}^{k,dir}(B^0 \& \bar{B}^0 \rightarrow \bar{f})$ and/or $\mathcal{A}_{CP}^{k,mix}(B^0 \& \bar{B}^0 \rightarrow f) \neq -\mathcal{A}_{CP}^{k,mix}(B^0 \& \bar{B}^0 \rightarrow \bar{f})$.

2.4 Input Parameters

The input parameters are collected in Table I. In our numerical results, we will use the input parameters which are varied randomly within 1σ range. The Wilson coefficients C_i are evaluated at scales $\mu = m_b$ [39]. For hard spectator scattering, we take $\mu_h = \sqrt{\Lambda_{QCD} m_b}$. When we study the RPV effects, we consider only one RPV coupling product to contribute at one time, neglecting the interferences between different RPV coupling products, but keeping their

¹ We use a similar sign convention to that of [45] for self-tagging B^0 and charged B decays.

interferences with the SM amplitude. We assume that the masses of the sfermions are 100 GeV. For other values of the sfermion masses, the bounds on the couplings derived in this paper can be easily obtained by scaling them by factor $\tilde{f}^2 \equiv (\frac{m_{\tilde{f}}}{100 \text{ GeV}})^2$.

3 Numerical results and Analysis

Now we are ready to present our numerical results and analysis. First, we will show our estimations in the SM with the parameters listed in Table I and compare with the relevant experimental data. Then, we will consider the RPV effects and constrain the relevant RPV couplings from the experimental data. Using the constrained parameter spaces, we will give

Table I: Default values of the input parameters and the $\pm 1\sigma$ error ranges for the sensitive parameters used in our numerical calculations.

$m_{B_s} = 5.366 \text{ GeV}, m_{K^{*\pm}} = 0.892 \text{ GeV}, m_{K^\pm} = 0.494 \text{ GeV},$ $m_{\pi^\pm} = 0.140 \text{ GeV}, m_\rho = 0.775 \text{ GeV}, \overline{m}_b(\overline{m}_b) = (4.20 \pm 0.07) \text{ GeV},$ $\overline{m}_u(2\text{GeV}) = (0.0015 \sim 0.003) \text{ GeV}, \overline{m}_d(2\text{GeV}) = (0.003 \sim 0.007) \text{ GeV},$ $\overline{m}_s(2\text{GeV}) = (0.095 \pm 0.025) \text{ GeV}, \tau_{B_d} = (1.530 \pm 0.009) \text{ ps}, \tau_{B_s} = (1.437_{-0.031}^{+0.030}) \text{ ps}.$	[46]
$ V_{ud} = 0.97430 \pm 0.00019, V_{us} = 0.22521_{-0.00082}^{+0.00083}, V_{ub} = 0.00344_{-0.00017}^{+0.00022},$ $ V_{cd} = 0.22508_{-0.00082}^{+0.00084}, V_{cs} = 0.97350_{-0.00022}^{+0.00021}, V_{cb} = 0.04045_{-0.00078}^{+0.00106},$ $ V_{td} = 0.00841_{-0.00092}^{+0.00035}, V_{ts} = 0.03972_{-0.00077}^{+0.00115}, V_{tb} = 0.999176_{-0.000044}^{+0.000031},$ $\alpha = (90.7_{-2.9}^{+4.5})^\circ, \beta = (21.7_{-0.9}^{+1.0})^\circ, \gamma = (67.6_{-4.5}^{+2.8})^\circ.$	[47]
$f_K = 0.160 \text{ GeV}, f_{K^*} = (0.217 \pm 0.005) \text{ GeV}, f_{K^*}^\perp = (0.156 \pm 0.010) \text{ GeV},$ $f_\pi = 0.131 \text{ GeV}, f_\rho = (0.205 \pm 0.009) \text{ GeV}, f_\rho^\perp = (0.147 \pm 0.010) \text{ GeV},$ $A_0^{B_s \rightarrow K^*}(0) = 0.360 \pm 0.034, A_1^{B_s \rightarrow K^*}(0) = 0.233 \pm 0.022, A_2^{B_s \rightarrow K^*}(0) = 0.181 \pm 0.025,$ $V^{B_s \rightarrow K^*}(0) = 0.311 \pm 0.026, F_0^{B_s \rightarrow K}(0) = 0.30_{-0.03}^{+0.04}.$	[48, 49]
$f_{B_s} = (0.245 \pm 0.025) \text{ GeV}.$	[50]
$\lambda_B = (0.46 \pm 0.11) \text{ GeV}.$	[51]
$\alpha_1^\pi = 0, \alpha_2^\pi = 0.20 \pm 0.15, \alpha_1^\rho = 0, \alpha_2^\rho = 0.1 \pm 0.2,$ $\alpha_1^K = 0.2 \pm 0.2, \alpha_2^K = 0.1 \pm 0.3, \alpha_1^{K^*} = 0.06 \pm 0.06, \alpha_2^{K^*} = 0.1 \pm 0.2.$	[6, 13]

the RPV SUSY predictions for the branching ratios, the CP asymmetries and the longitudinal polarization fractions, which have not been measured yet in $B_s \rightarrow K^{(*)-} K^{(*)+}$, $K^{(*)-} \pi^+$, $K^{(*)-} \rho^+$ systems.

For CP case (i) decays $B_s \rightarrow K^{(*)-} \pi^+$ and $K^{(*)-} \rho^+$, we will study the CP averaged branching ratios (\mathcal{B}), \mathcal{A}_{CP}^{dir} and the longitudinal polarization fractions (f_L). For CP cases (ii), (iii) and (iv) decays $B_s \rightarrow K^{(*)-} K^{(*)+}$, we will also study \mathcal{A}_{CP}^{mix} besides \mathcal{B} , \mathcal{A}_{CP}^{dir} and f_L . For CPA of $B_s \rightarrow K^{*-} K^{*+}$, $K^{*-} \rho^+$, we only study the longitudinal direct CPA ($\mathcal{A}_{CP}^{L,dir}$) and longitudinal mixing-induced CPA ($\mathcal{A}_{CP}^{L,mix}$). The numerical results in the SM are presented in Table II. The detailed error estimates corresponding to the different types of theoretical uncertainties have been already studied in Refs. [6, 13], and our SM results of \mathcal{B} , \mathcal{A}_{CP}^{dir} and f_L are consistent with the ones in Refs. [6, 13].

Table II: The SM predictions for \mathcal{B} (in units of 10^{-5}), \mathcal{A}_{CP}^{dir} , and \mathcal{A}_{CP}^{mix} in $B_s \rightarrow K^- K^+$, $K^{*-} K^+$, $K^- K^{*+}$, $K^- \pi^+$, $K^{*-} \pi^+$, $K^- \rho^+$ decays within QCDF. $B_s \& \bar{B}_s \rightarrow K^{*-} K^+$ denotes that B_s^0 and \bar{B}_s^0 decay to the same final state $K^{*-} K^+$.

Decay modes	\mathcal{B}	\mathcal{A}_{CP}^{dir}	\mathcal{A}_{CP}^{mix}
$B_s \rightarrow K^- K^+$	[0.89, 4.45]	[0.02, 0.06]	[0.21, 0.43]
$B_s \rightarrow K^{*-} K^+$	[0.22, 2.14]	[-0.07, 0.02]	
$B_s \rightarrow K^- K^{*+}$	[0.21, 0.65]	[0.03, 0.10]	
$B_s \& \bar{B}_s \rightarrow K^{*-} K^+$		[-0.72, 0.34]	[-0.30, 0.04]
$B_s \& \bar{B}_s \rightarrow K^- K^{*+}$		[-0.31, 0.73]	[-0.34, 0.12]
$B_s \rightarrow K^- \pi^+$	[0.61, 1.47]	[-0.09, -0.05]	
$B_s \rightarrow K^{*-} \pi^+$	[0.84, 1.72]	[0.00, 0.02]	
$B_s \rightarrow K^- \rho^+$	[1.33, 3.51]	[-0.02, -0.01]	

- Our results of $B \rightarrow PP$ and PV are obtained excluding the uncertainties of power corrections parameterized by the quantities X_A and X_H . In the QCDF, the endpoint divergent integrals appear in the hard-scattering contributions and in the weak annihilation contributions, which are treated with model-dependent parameters [6] $X_H \equiv (1 + \varrho_H e^{i\varphi_H}) \ln \frac{m_B}{\Lambda_h}$ and $X_A \equiv (1 + \varrho_A e^{i\varphi_A}) \ln \frac{m_B}{\Lambda_h}$, respectively. The different X_A values are allowed for the

Table III: The SM predictions for \mathcal{B} (in units of 10^{-5}), $\mathcal{A}_{CP}^{L,dir}$, $\mathcal{A}_{CP}^{L,mix}$ and f_L in $B_s \rightarrow K^{*-}K^{*+}$, $K^{*-}\rho^+$ decays within QCDF.

Decay modes	\mathcal{B}	$\mathcal{A}_{CP}^{L,dir}$	$\mathcal{A}_{CP}^{L,mix}$	f_L
$B_s \rightarrow K^{*-}K^{*+}$	[0.39, 1.71]	[-0.04, 0.19]	[0.70, 0.93]	[0.38, 0.89]
$B_s \rightarrow K^{*-}\rho^+$	[1.03, 6.23]	[-0.06, -0.03]		[0.86, 0.97]

four cases PP , PV , VP and VV . Our results of $B \rightarrow PP, PV$ are obtained without the uncertainties of power corrections and set $\varrho_A = \varrho_H = 0$. For two vector final-state meson decays, in order to be consistent with the longitudinal polarization fractions around 0.5 in the penguin-dominated decays $B \rightarrow \phi K^{*0}$ and $\rho^+ K^{*0}$, maximal annihilation contribution are considered ($\varrho_A = 0.6$ and $\varphi_A = -40^\circ$) in Ref. [13]. We also consider the large annihilation contribution and suggest $\varrho_H = 0$, $\varrho_A = 0.6 \pm 0.2$ and $\varphi_A = (-40 \pm 10)^\circ$. The annihilation topology obviously contributes to \mathcal{B} , $\mathcal{A}_{CP}^{L,dir}$ and $\mathcal{A}_{CP}^{L,mix}$ besides f_L in $B_s \rightarrow K^{*-}K^{*+}$ decay. For example, $\mathcal{A}_{CP}^{L,dir}(B_s^0 \rightarrow K^{*-}K^{*+})$ receives much larger annihilation contribution than $\mathcal{A}_{CP}^{dir}(B_s^0 \rightarrow K^-K^+)$ does. It is also noted that annihilation contribution could cancel voluminous penguin contribution in $\mathcal{A}_{CP}^{L,dir}(B_s^0 \rightarrow K^{*-}K^{*+})$.

- For CP case (iv) $B_s \rightarrow K^{*-}K^+$ decay, the final state can come both from a pure B_s and a pure \bar{B}_s , the amplitudes for the direct decay $B_s \rightarrow K^{*-}K^+$ and the mixing-induced sequence $B_s \rightarrow \bar{B}_s \rightarrow K^{*-}K^+$. We obtain $\mathcal{A}_{CP}^{dir}(B_s \& \bar{B}_s \rightarrow K^{*-}K^+) \approx -\mathcal{A}_{CP}^{dir}(B_s \& \bar{B}_s \rightarrow K^-K^{*+})$, however, $\mathcal{A}_{CP}^{mix}(B_s \& \bar{B}_s \rightarrow K^{*-}K^+) \neq -\mathcal{A}_{CP}^{mix}(B_s \& \bar{B}_s \rightarrow K^-K^{*+})$, which imply that its direct CP violation is very small, nevertheless its CP violating effect can appear through the interference of the direct decay $B_s \rightarrow K^{*-}K^+$ and the mixing-induced decay $B_s \rightarrow \bar{B}_s \rightarrow K^{*-}K^+$. In addition, the theoretical predictions for above CP asymmetry parameters suffer large uncertainties, which are dominated by the uncertainties of mass and the Gegenbauer moments in the expansion of the light-cone distribution amplitudes, and also due to the uncertainties of the form factors and the CKM matrix elements.
- In penguin-dominated decay $B_s^0 \rightarrow K^{*+}K^{*-}$, as transverse and longitudinal contributions can be of the similar magnitude, the CP asymmetry and the polarization fractions predictions will suffer large uncertainties. For example, compared to $\mathcal{A}_{CP}^{dir}(B_s^0 \rightarrow K^-K^+)$,

$\mathcal{A}_{CP}^{L,dir}(B_s^0 \rightarrow K^{*-}K^{*+})$ suffers quite large uncertainties, which mostly come from the uncertainties of the relevant form factors and the weak annihilation parameter X_A . $f_L(B_s^0 \rightarrow K^{*-}K^{*+})$ has quite large allowed range for the same reason as $\mathcal{A}_{CP}^{L,dir}(B_s^0 \rightarrow K^{*-}K^{*+})$.

- $\mathcal{A}_{CP}^{L,mix}(B_s^0 \rightarrow K^{*-}K^{*+})$ is much larger than $\mathcal{A}_{CP}^{mix}(B_s^0 \rightarrow K^-K^+)$ in the SM. Large difference between them arises from chirally-enhanced terms, which give large contribution to penguin-dominated decay modes with pseudoscalar final-states.
- For the color-allowed tree-dominated decays $B_s \rightarrow K^-\pi^+$, $K^{*-}\pi^+$, $K^-\rho^+$, and $K^{*-}\rho^+$, power corrections have limited impact, and the main sources of theoretical uncertainties in the branching ratio are CKM matrix elements and form factors. Their A_{CP}^{dir} and $A_{CP}^{L,dir}$ can be predicted quite precisely, and found to be very small ($\sim 10^{-2}$) due to small penguin amplitudes. The uncertainty of $f_L(B_s \rightarrow K^{*-}\rho^+)$ is mostly due to the uncertainties of form factors.

Now we turn to the RPV effects in $B_s \rightarrow K^{(*)-}K^{(*)+}$, $K^{(*)-}\pi^+$, and $K^{(*)-}\rho^+$ decays. There are two RPV coupling products, $\lambda_{131}''^* \lambda_{121}''$ and $\lambda_{i13}^* \lambda'_{i12}$ contributing to four $B_s \rightarrow K^{(*)-}K^{(*)+}$ modes, which involve the quark level process $b \rightarrow u\bar{u}s$. Four decays $B_s \rightarrow K^{(*)-}\pi^+$, $K^{(*)-}\rho^+$ are due to $b \rightarrow u\bar{u}d$ at the quark level, and the relevant RPV coupling products are $\lambda_{132}''^* \lambda_{112}''$ and $\lambda_{i13}^* \lambda'_{i11}$. We use the experimental results shown in Eq. (1) to constrain the relevant RPV parameters.

Our bounds on $\lambda_{131}''^* \lambda_{121}''$ and $\lambda_{i13}^* \lambda'_{i12}$ are demonstrated in Fig. 2 (a-b) by using the experimental measurement of $\mathcal{B}(B_s \rightarrow K^-K^+)$ within 1σ error-bar range. From Fig. 2 (a-b), we find that the RPV weak phases of $\lambda_{131}''^* \lambda_{121}''$ and $\lambda_{i13}^* \lambda'_{i12}$ are not much constrained, but the modulus of the two RPV coupling products can be tightly upper limited. Since the SM prediction ranges of $\mathcal{A}_{CP}^{dir}(\mathcal{B})$ in $B_s \rightarrow K^-\pi^+$ decay summarized in Table II is a little smaller (larger) than the corresponding measurements within 1σ by CDF shown in Eq. (1), the allowed ranges of $\lambda_{132}''^* \lambda_{112}''$ and $\lambda_{i13}^* \lambda'_{i11}$ are strongly restricted by these experimental data. We obtain $|\lambda_{132}''^* \lambda_{112}''| \in [0.22, 4.86] \times 10^{-3}$ and its phase $\phi_{RPV} \in [80^\circ, 123^\circ]$. However, we could not find the allowed space of $\lambda_{i13}^* \lambda'_{i11}$ within 1σ error-bar of the experimental bounds. Within 2σ error-bar of the experimental data, one can find the allowed spaces of these two RPV coupling products which are given in Fig. 2 (c-d). One can find that the RPV weak phases only

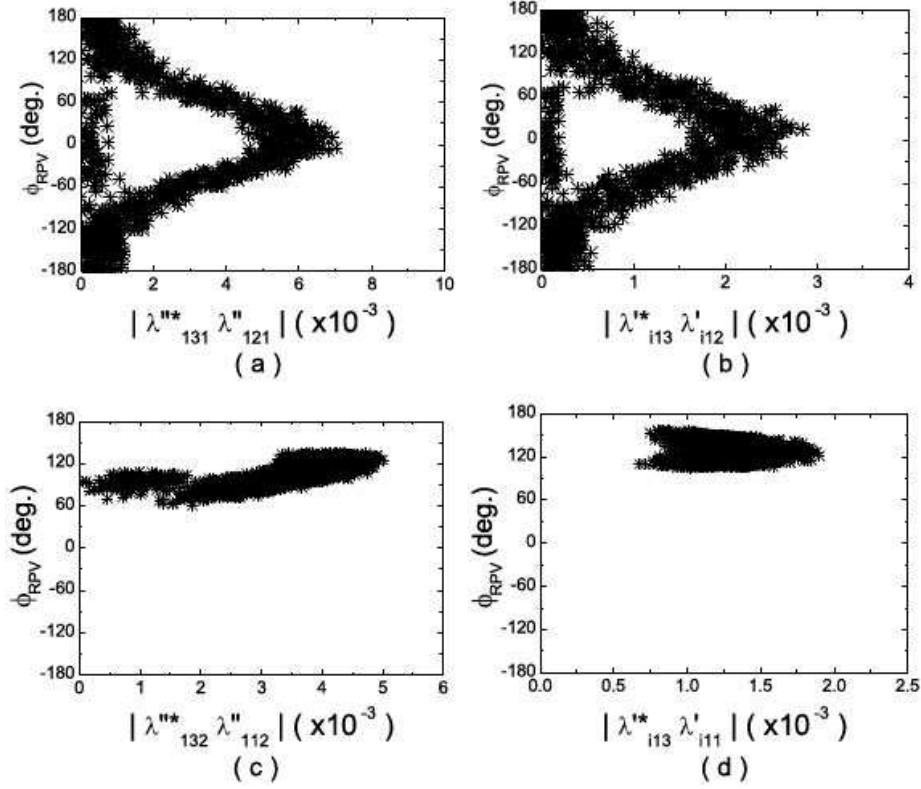


Figure 2: The allowed parameter spaces for the relevant RPV couplings constrained by $B_s \rightarrow K^- K^+$ and $K^- \pi^+$. ϕ_{RPV} denotes the RPV weak phase.

Table IV: Bounds on the relevant RPV couplings by $B_s \rightarrow K^- K^+$, $K^- \pi^+$ decays for 100 GeV sfermions. Previous bounds are listed for comparison.

Couplings	Our bounds [Process]	Bounds I [Process] [29]	Bounds II [Process] [52]
$ \lambda''_{131} \lambda''_{121} $	$\leq 7.01 \times 10^{-3}$ [$B_s \rightarrow K^+ K^-$]	$[0.61, 4.6] \times 10^{-3}$ [$B \rightarrow \pi K$] $[5.6, 7.2] \times 10^{-3}$ [$B \rightarrow \pi K$]	$\leq 1.54 \times 10^{-2}$ [$B_u \rightarrow K^- \pi^0$]
$ \lambda'^*_{i13} \lambda'_{i12} $	$\leq 2.84 \times 10^{-3}$ [$B_s \rightarrow K^+ K^-$]	$[0.36, 1.1] \times 10^{-3}$ [$B \rightarrow \pi K$]	$\leq 2.71 \times 10^{-3}$ [$B_u \rightarrow K^- \pi^0$]
$ \lambda''_{132} \lambda''_{112} $	$\leq 5.01 \times 10^{-3}$ [$B_s \rightarrow K^+ \pi^-$]	$[0.54, 2.9] \times 10^{-3}$ [$B_d \rightarrow \pi \pi$]	$\leq 4.69 \times 10^{-3}$ [$B_d \rightarrow \pi^+ \pi^-$]
$ \lambda'^*_{i13} \lambda'_{i11} $	$[0.67, 1.90] \times 10^{-3}$ [$B_s \rightarrow K^+ \pi^-$]	$[0.27, 0.77] \times 10^{-3}$ [$B_d \rightarrow \pi \pi$]	$\leq 1.90 \times 10^{-3}$ [$B_d \rightarrow \pi^- \pi^+$]

have the positive values, the RPV weak phase of $\lambda''_{132} \lambda''_{112}$ lies in $[60^\circ, 139^\circ]$ and the phase of $\lambda'^*_{i13} \lambda'_{i11}$ lies in $[104^\circ, 158^\circ]$. Furthermore, the strengths of the two RPV coupling products are restricted strongly, which are summarized in Table IV. For comparison, the existing bounds on these quadric coupling products, which obtain from $B_{u,d}$ decays of the same quark level process [29, 52] are also listed. Note that, previous bounds-I of Ref. [29] are obtained by considering the experimental constraints of all relevant decay modes at the same time, so the allowed RPV

coupling spaces are very narrow. In Ref. [52], the bounds are given through experimental restraints mode by mode. Our bounds on $\lambda''_{131}\lambda''_{121}$, $\lambda'_{i13}\lambda'_{i12}$ and $\lambda''_{132}\lambda''_{112}$ are consistent with the existing ones in Refs. [52], and just a little weaker than these in Ref. [29] which are obtained from many correlated experimental constraints. Our bound of $|\lambda'_{i13}\lambda'_{i11}|$ also consists with one from Ref. [52], however, there is only very narrow overlap between range $[0.27, 0.77] \times 10^{-3}$ in Ref. [29] and ours $[0.67, 1.90] \times 10^{-3}$, therefore, it should be of order 10^{-4} if $|\lambda'_{i13}\lambda'_{i11}|$ can survive.

Next, we will use the constrained parameter spaces from $B_s \rightarrow K^- K^+$ and $K^- \pi^+$ decays, as shown in Fig. 2, to predict the RPV effects on the other quantities which have not been measured yet in $B_s \rightarrow K^{(*)-} K^{(*)+}$, $K^{(*)-} \pi^+$ and $K^{(*)-} \rho^+$ decays. With the expressions for \mathcal{B} , \mathcal{A}_{CP}^{dir} , \mathcal{A}_{CP}^{mix} and f_L , we perform a scan through the input parameters and the new constrained RPV coupling spaces, and then the allowed ranges for \mathcal{B} , \mathcal{A}_{CP}^{dir} , \mathcal{A}_{CP}^{mix} and f_L are obtained with different RPV couplings, which satisfy relevant experimental constraints of B_s decays given in Eq. (1). The numerical results for $B_s \rightarrow K^{(*)-} K^{(*)+}$ and $B_s \rightarrow K^{(*)-} \pi^+$, $K^{(*)-} \rho^+$ are summarized in Table V and Table VI, respectively.

Comparing the RPV SUSY predictions given in Table V and Table VI to the SM values listed in Table II and Table III, we give some remarks on the numerical results.

- All branching ratios can be greatly changed by the RPV couplings compared to the SM expectations.
- The RPV effects on $\mathcal{A}_{CP}^{dir}(B_s \rightarrow K^{*-} \pi^+)$ and $\mathcal{A}_{CP}^{dir}(B_s \rightarrow K^- \rho^+)$ are found to be very small, but could be large for the direct CPA in other five $B_s \rightarrow K^{*-} \rho^+$ and $K^{(*)-} K^{(*)+}$ decays.
- The mixing-induced CPA in $B_s \rightarrow K^{(*)-} K^{(*)+}$ system can be greatly enhanced by the RPV couplings $\lambda''_{131}\lambda''_{121}$ and $\lambda'_{i13}\lambda'_{i12}$.
- The squark exchange couplings $\lambda''_{131}\lambda''_{121}$ and $\lambda''_{132}\lambda''_{112}$ could have significant impacts on $f_L(B_s \rightarrow K^{*-} K^{*+})$ and $f_L(B_s \rightarrow K^{*-} \rho^+)$, which could be decreased as low as 0.30 and 0.42, respectively.

In Figs. 3-6, we present correlations between the physical observable \mathcal{B} , \mathcal{A}_{CP}^{dir} , \mathcal{A}_{CP}^{mix} , f_L and the parameter spaces of different RPV couplings by these three-dimensional scatter plots.

Table V: The theoretical predictions of $B_s \rightarrow K^{(*)-} K^{(*)+}$ for \mathcal{B} (in units of 10^{-5}), \mathcal{A}_{CP}^{dir} , \mathcal{A}_{CP}^{mix} and f_L with the allowed regions of the different RPV couplings.

	$\lambda''_{131} \lambda''_{121}$	$\lambda'_{i12} \lambda'_{i13}$
$\mathcal{B}(B_s \rightarrow K^{*-} K^+)$	[0.33, 10.56]	[0.32, 12.89]
$\mathcal{B}(B_s \rightarrow K^- K^{*+})$	[0.01, 28.88]	
$\mathcal{B}(B_s \rightarrow K^{*-} K^{*+})$	[0.29, 27.23]	
$\mathcal{A}_{CP}^{dir}(B_s \rightarrow K^- K^+)$	[-0.50, 0.50]	[-0.25, 0.23]
$\mathcal{A}_{CP}^{dir}(B_s \rightarrow K^{*-} K^+)$	[-0.25, 0.50]	[-0.11, 0.22]
$\mathcal{A}_{CP}^{dir}(B_s \rightarrow K^- K^{*+})$	[-0.98, 0.95]	
$\mathcal{A}_{CP}^{L, dir}(B_s \rightarrow K^{*-} K^{*+})$	[-0.30, 0.52]	
$\mathcal{A}_{CP}^{mix}(B_s \rightarrow K^- K^+)$	[-0.97, 0.98]	[-0.99, 1.00]
$\mathcal{A}_{CP}^{mix}(B_s \& \bar{B}_s \rightarrow K^{*-} K^+)$	[-0.89, 0.97]	[-0.98, 0.55]
$\mathcal{A}_{CP}^{mix}(B_s \& \bar{B}_s \rightarrow K^- K^{*+})$	[-0.89, 0.96]	[-0.98, 0.58]
$\mathcal{A}_{CP}^{L, mix}(B_s \rightarrow K^{*-} K^{*+})$	[-1.00, 1.00]	
$f_L(B_s \rightarrow K^{*-} K^{*+})$	[0.30, 0.97]	

Table VI: The theoretical predictions of $B_s \rightarrow K^{(*)-} \pi^+, K^{(*)-} \rho^+$ for \mathcal{B} (in units of 10^{-5}), \mathcal{A}_{CP}^{dir} and f_L with the allowed regions of the different RPV couplings.

	$\lambda''_{132} \lambda''_{112}$	$\lambda'_{i13} \lambda'_{i11}$
$\mathcal{B}(B_s \rightarrow K^{*-} \pi^+)$	[1.34, 11.59]	[4.49, 13.47]
$\mathcal{B}(B_s \rightarrow K^- \rho^+)$	[2.02, 23.32]	
$\mathcal{B}(B_s \rightarrow K^{*-} \rho^+)$	[0.40, 3.31]	
$\mathcal{A}_{CP}^{dir}(B_s \rightarrow K^{*-} \pi^+)$	[-0.04, 0.04]	[0.00, 0.02]
$\mathcal{A}_{CP}^{dir}(B_s \rightarrow K^- \rho^+)$	[-0.05, 0.01]	
$\mathcal{A}_{CP}^{L, dir}(B_s \rightarrow K^{*-} \rho^+)$	[-0.25, 0.73]	
$f_L(B_s \rightarrow K^{*-} \rho^+)$	[0.42, 0.96]	

From Figs. 3-6, one can see the changing trends of the physical observables with the modulus and RPV weak phase ϕ_{RPV} . Taking the first plot in Fig. 3(a) as an example, this plot shows $\mathcal{B}(B_s \rightarrow K^{*-}K^+)$ changing trend with RPV coupling $\lambda_{131}''^* \lambda_{121}''$, where projections on three perpendicular planes are also given. The $|\lambda_{131}''^* \lambda_{121}''|$ - ϕ_{RPV} plane displays the allowed regions of $\lambda_{131}''^* \lambda_{121}''$ which satisfy experimental data in Eq. (1) (the same as the Fig.2(a)). The $\mathcal{B}(B_s \rightarrow K^{*-}K^+)$ - $|\lambda_{131}''^* \lambda_{121}''|$ plane shows that $\mathcal{B}(B_s \rightarrow K^{*-}K^+)$ is increasing with $|\lambda_{131}''^* \lambda_{121}''|$,

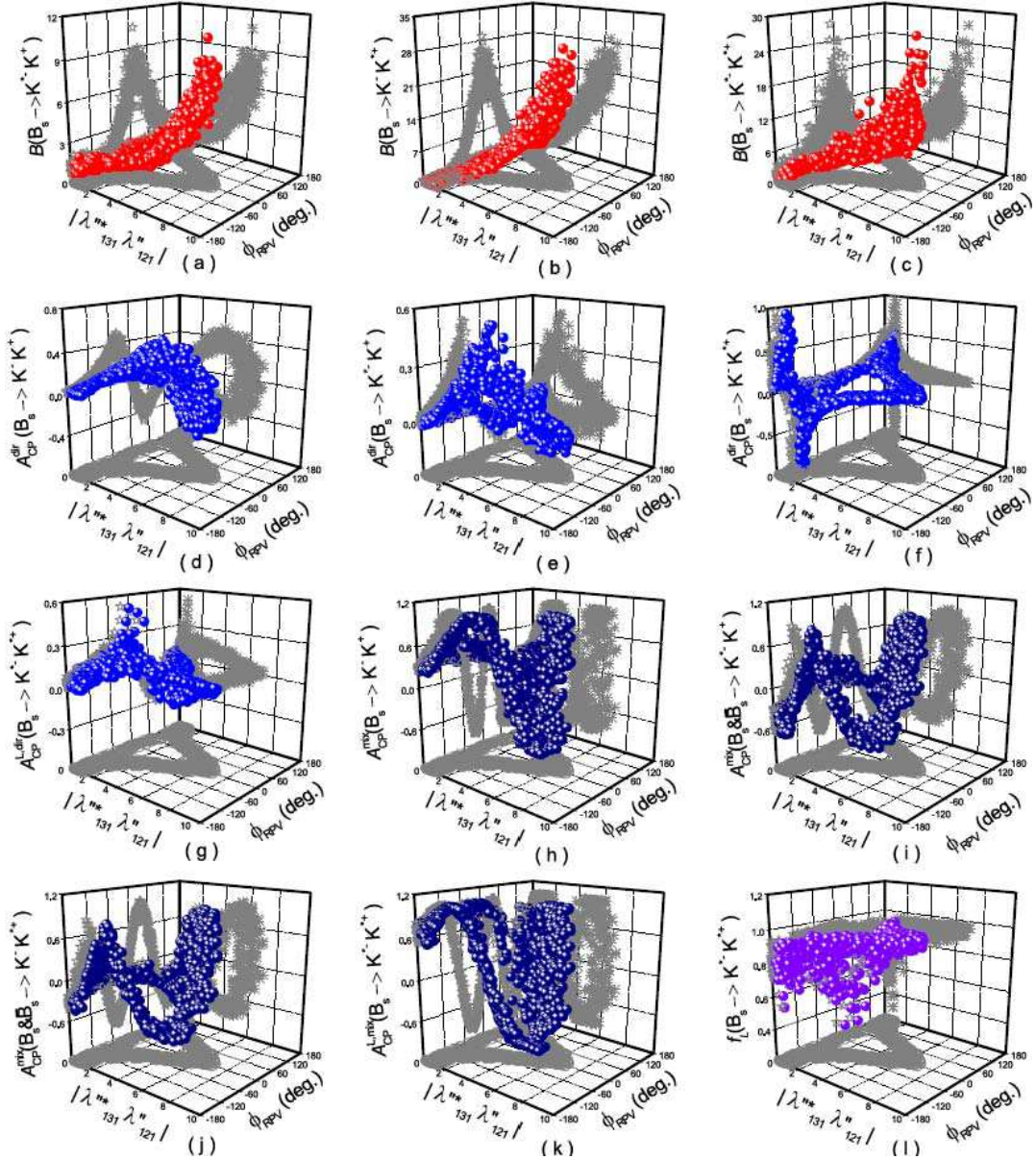


Figure 3: The effects of RPV coupling $\lambda_{131}''^* \lambda_{121}''$ in $B_s \rightarrow K^-K^+, K^-K^{*+}, K^{*-}K^+, K^{*-}K^{*+}$ decays. \mathcal{B} in units of 10^{-5} and $|\lambda_{131}''^* \lambda_{121}''|$ in units of 10^{-3} .

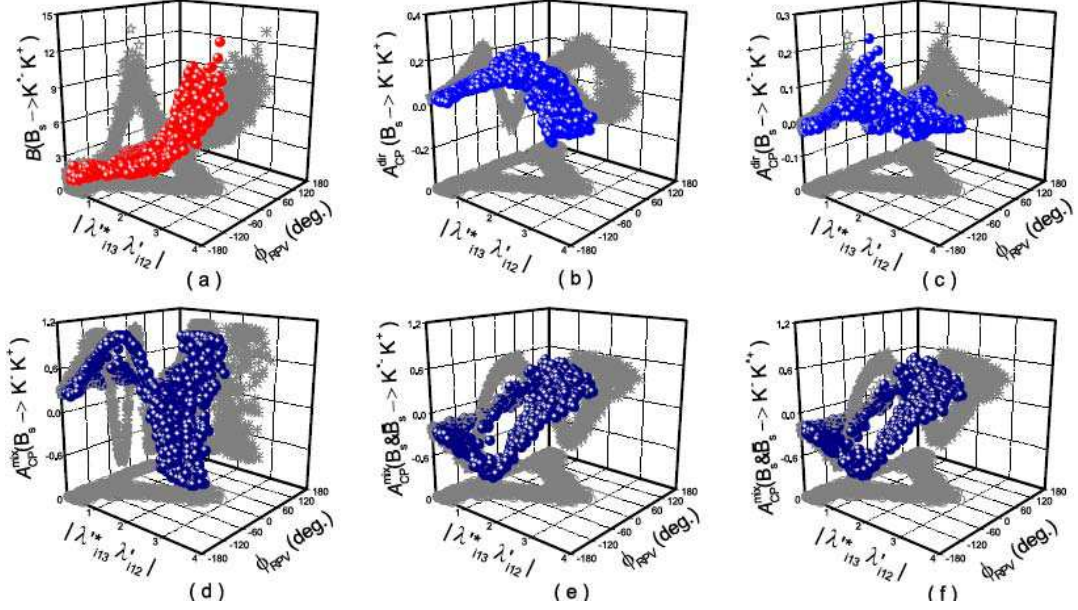


Figure 4: The effects of RPV coupling $\lambda'_{i13}\lambda'_{i12}$ in $B_s \rightarrow K^- K^+, K^- K^{*+}$ decays. \mathcal{B} in units of 10^{-5} and $|\lambda'_{i13}\lambda'_{i12}|$ in units of 10^{-3} .

the $\mathcal{B}(B_s \rightarrow K^{*-} K^+)$ - ϕ_{RPV} plane shows that $\mathcal{B}(B_s \rightarrow K^{*-} K^+)$ is decreasing with $|\phi_{RPV}|$. Additional refined measurements of $\mathcal{B}(B_s \rightarrow K^- K^+)$ can further restrict the constrained space of $\lambda''_{131}\lambda''_{121}$, thus more accurate $\mathcal{B}(B_s \rightarrow K^{*-} K^+)$ can be predicted. The following salient features in Figs. 3-6 are summarized as following.

- Fig.3 displays the effects of RPV coupling $\lambda''_{131}\lambda''_{121}$ on \mathcal{B} , \mathcal{A}_{CP}^{dir} , \mathcal{A}_{CP}^{mix} in penguin-dominated $B_s \rightarrow K^- K^+, K^- K^{*+}, K^{*-} K^+$ and \mathcal{B} , $\mathcal{A}_{CP}^{L,dir}$, $\mathcal{A}_{CP}^{L,mix}$, f_L in penguin-dominated $B_s \rightarrow K^{*-} K^{*+}$ decays. The constrained $|\lambda''_{131}\lambda''_{121}|$ - ϕ_{RPV} plane shows the allowed range of $\lambda''_{131}\lambda''_{121}$ as shown in Fig. 2(a). The $\mathcal{B}(B_s \rightarrow K^{*-} K^+, K^- K^{*+}, K^{*-} K^{*+})$ shown in Fig. 3(a-c) have the similar change trends with $|\lambda''_{131}\lambda''_{121}|$ and $|\phi_{RPV}|$, and they all increases with $|\lambda''_{131}\lambda''_{121}|$ and decreases with $|\phi_{RPV}|$. For the $\mathcal{A}_{CP}^{dir}/\mathcal{A}_{CP}^{L,dir}$ shown in Fig. 3(d-g), $\lambda''_{131}\lambda''_{121}$ coupling contribution could be significant. $|\mathcal{A}_{CP}^{dir}(B_s \rightarrow K^- K^+)|$ increases when $|\lambda''_{131}\lambda''_{121}|$ is small, then $\mathcal{A}_{CP}^{dir}(B_s \rightarrow K^- K^+)$ decreases and its sign is flipped. $\mathcal{A}_{CP}^{dir}(B_s(\bar{B}_s) \rightarrow K^{*-} K^+)$, $\mathcal{A}_{CP}^{dir}(B_s(\bar{B}_s) \rightarrow K^- K^{*+})$ and $\mathcal{A}_{CP}^{L,dir}(B_s \rightarrow K^{*-} K^{*+})$ could have smaller range with $|\lambda''_{131}\lambda''_{121}|$. $|\mathcal{A}_{CP}^{dir}(B_s \rightarrow K^- K^+, K^{*-} K^+)|$ and $|\mathcal{A}_{CP}^{L,dir}(B_s \rightarrow K^{*-} K^{*+})|$ decrease with $|\phi_{RPV}|$. $\mathcal{A}_{CP}^{dir}(B_s \rightarrow K^{*-} K^+, K^- K^{*+})$ and $\mathcal{A}_{CP}^{L,dir}(B_s \rightarrow K^{*-} K^{*+})$ could be close to zero in entire ϕ_{RPV} range. As shown in Fig. 3(h-k), four mixing-induced

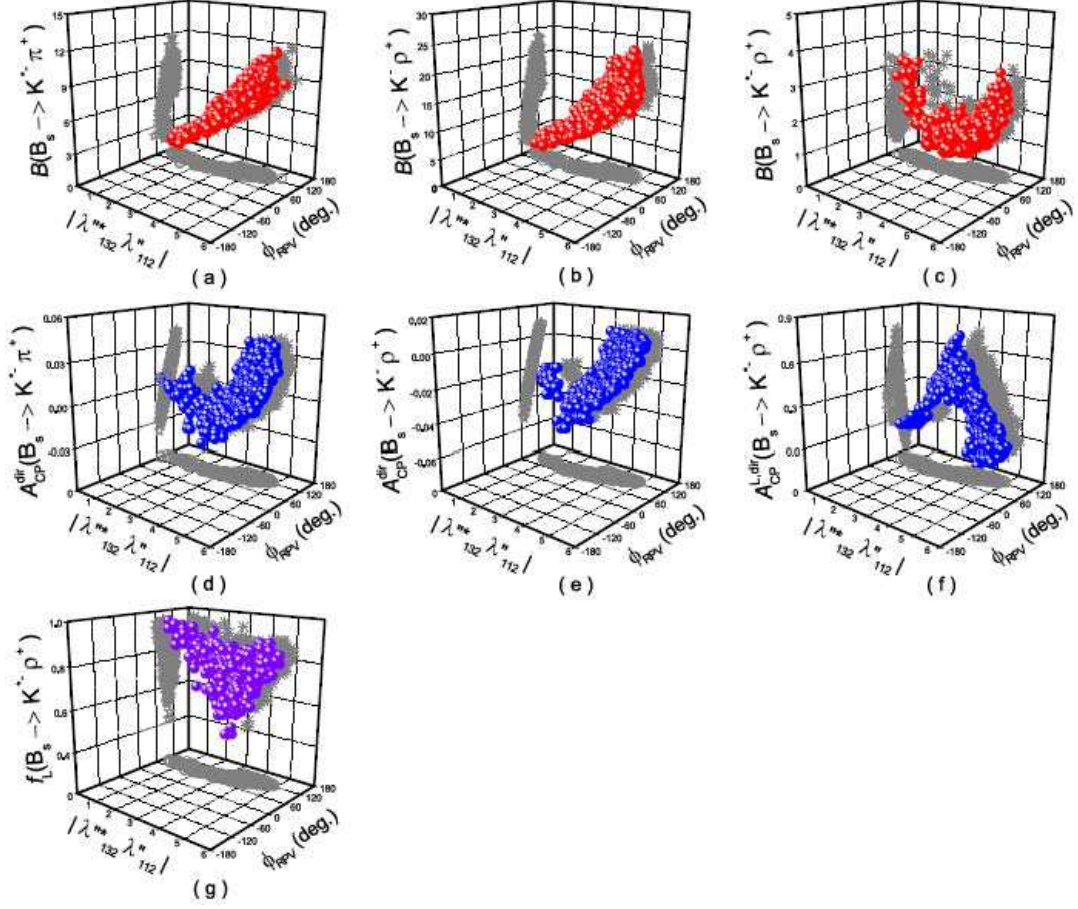


Figure 5: The effects of RPV coupling $\lambda''^*_{132}\lambda''_{112}$ in $B_s \rightarrow K^*\pi^+$, $K^-\rho^+$, $K^*\rho^+$ decays. \mathcal{B} in units of 10^{-5} and $|\lambda''^*_{132}\lambda''_{112}|$ in units of 10^{-3} .

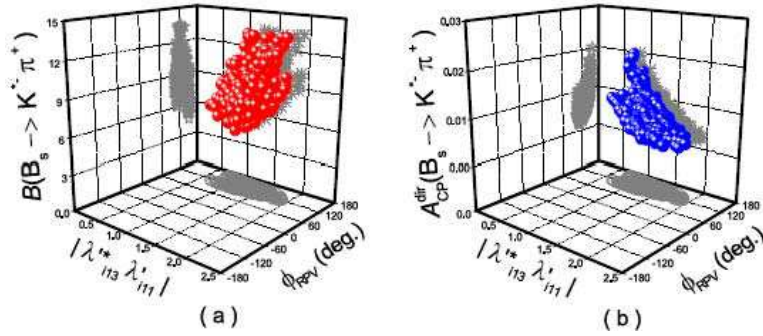


Figure 6: The effects of RPV coupling $\lambda^*_{i11}\lambda'_{i13}$ in $B \rightarrow K^*\pi^+$ decays. \mathcal{B} in units of 10^{-5} and $|\lambda^*_{i11}\lambda'_{i13}|$ in units of 10^{-3} .

CP asymmetries are very sensitive to $|\phi_{RPV}|$ but not sensitive to $|\lambda''^*_{131}\lambda''_{121}|$. For the penguin dominated process $B_s \rightarrow K^*K^{*+}$, its longitudinal polarization could be small as shown in Fig. 3(l), however, most points of $f_L(B_s \rightarrow K^*K^{*+})$ fill in $[0.7, 0.9]$.

- The effects of $\lambda'_{i13}\lambda'_{i12}$ on \mathcal{B} , \mathcal{A}_{CP}^{dir} and \mathcal{A}_{CP}^{mix} of $B_s \rightarrow K^-K^+, K^{*-}K^+, K^-K^{*+}$ are presented in Fig. 4. The constrained $|\lambda'_{i23}\lambda'_{i12}|$ - ϕ_{RPV} plane is the same as Fig. 2(b). Fig. 4(a) show that $\mathcal{B}(B_s \rightarrow K^{*-}K^+)$ increases with $|\lambda'_{i13}\lambda'_{i12}|$ and decreases with $|\phi_{RPV}|$. As shown in Fig. 4(b), at first $|\mathcal{A}_{CP}^{dir}(B_s \rightarrow K^-K^+)|$ increase with $|\lambda'_{i13}\lambda'_{i12}|$, then $\mathcal{A}_{CP}^{dir}(B_s \rightarrow K^-K^+)$ could occupy the entire range $[-0.25, 0.23]$ when $|\lambda'_{i13}\lambda'_{i12}|$ lies in $[1.6, 2.8] \times 10^{-3}$, and $|\mathcal{A}_{CP}^{dir}(B_s \rightarrow K^-K^+)|$ decreases with $|\phi_{RPV}|$. $\mathcal{A}_{CP}^{dir}(B_s \rightarrow K^{*-}K^+)$ has narrow ranges with the constrained $|\lambda'_{i13}\lambda'_{i12}|$ and $|\phi_{RPV}|$. Fig. 4(d-f) show the RPV effects in relevant mixing-induced CPA. $|\mathcal{A}_{CP}^{mix}(B_s \rightarrow K^-K^+)|$ is not sensitive to $|\lambda'_{i13}\lambda'_{i12}|$ but sensitive to ϕ_{RPV} . $|\mathcal{A}_{CP}^{mix}(B_s \& \bar{B}_s \rightarrow K^{*-}K^+)|$ and $|\mathcal{A}_{CP}^{mix}(B_s \& \bar{B}_s \rightarrow K^-K^{*+})|$ decrease with $|\lambda'_{i13}\lambda'_{i12}|$ and they first increase and then decrease with $|\phi_{RPV}|$.
- In Fig. 5, we plot \mathcal{B} , \mathcal{A}_{CP}^{dir} of $B_s \rightarrow K^{*-}\pi^+, K^-\rho^+$, and \mathcal{B} , $\mathcal{A}_{CP}^{L,dir}$, f_L of $B_s \rightarrow K^{*-}\rho^+$ decays as functions of $\lambda''_{132}\lambda''_{112}$. The constrained $|\lambda''_{132}\lambda''_{112}|$ - ϕ_{RPV} plane is the same as Fig. 2(c). One can find $\mathcal{B}(B_s \rightarrow K^{*-}\pi^+, K^-\rho^+)$ increase with $|\lambda''_{132}\lambda''_{112}|$ and $|\phi_{RPV}|$. $\mathcal{B}(B_s \rightarrow K^{*-}\rho^+)$ first decreases and then increases with $|\lambda''_{132}\lambda''_{112}|$, and it is not very sensitive to $|\phi_{RPV}|$. As shown by Fig. 5(d-e), the squark exchange RPV effects on $\mathcal{A}_{CP}^{dir}(B \rightarrow K^{*-}\pi^+, K^-\rho^+)$ are very small. $\mathcal{A}_{CP}^{dir}(B \rightarrow K^{*-}\pi^+, K^-\rho^+)$ first decrease and then increase with $|\lambda''_{132}\lambda''_{112}|$, and they both increase with ϕ_{RPV} . $\mathcal{A}_{CP}^{L,dir}(B \rightarrow K^{*-}\rho^+)$ is sensitive to $\lambda''_{132}\lambda''_{112}$ coupling, and could be enhanced to $\sim 70\%$ when $|\lambda''_{132}\lambda''_{112}|$ is around 3×10^{-3} . $\mathcal{A}_{CP}^{L,dir}(B \rightarrow K^{*-}\rho^+)$ first increases and then decreases with $|\lambda''_{132}\lambda''_{112}|$, but is not sensitive to ϕ_{RPV} . $f_L(B \rightarrow K^{*-}\rho^+)$ has the largest allowed range when $|\lambda''_{132}\lambda''_{112}|$ is around 3×10^{-3} . The $\lambda''_{132}\lambda''_{112}$ couplings could decrease $f_L(B \rightarrow K^{*-}\rho^+)$ to 0.42.
- Fig. 6 shows the effects of the RPV couplings $\lambda'_{i13}\lambda'_{i11}$ in $B_s \rightarrow K^{*-}\pi^+$ decay. $\mathcal{B}(B_s \rightarrow K^{*-}\pi^+)$ increases with $|\lambda'_{i13}\lambda'_{i11}|$ and is insensitive to ϕ_{RPV} . $\mathcal{A}_{CP}^{dir}(B \rightarrow K^{*-}\pi^+)$ decreases with $|\lambda'_{i13}\lambda'_{i11}|$ and increases with ϕ_{RPV} .

4 Conclusions

In conclusion, we have studied the eight decay modes $B_s \rightarrow K^{(*)-}K^{(*)+}$, $K^{(*)-}\pi^+$, $K^{(*)-}\rho^+$ in the RPV SUSY with the QCDF for the hadronic dynamics. With the recent experimental data of B_s decays, we have obtained fairly constrained parameter spaces of the RPV couplings.

Furthermore, using the constrained parameter spaces, we have shown the RPV SUSY expectations for the other quantities in $B_s \rightarrow K^{(*)-}K^{(*)+}$, $K^{(*)-}\pi^+$, $K^{(*)-}\rho^+$ decays which have not been measured yet.

We have found that the RPV couplings $\lambda''_{131}\lambda''_{121}$ and $\lambda'_{i13}\lambda'_{i12}$ could significantly affect penguin-dominated $B_s \rightarrow K^{(*)-}K^{(*)+}$ decays. Within the parameter spaces already highly constrained by $B_s \rightarrow K^-K^+$, the branching ratios of $B_s \rightarrow K^-K^{*+}$, $K^{*-}K^+$ and $K^{*-}K^{*+}$ could be enhanced by few times, and the direct CPA and the mixing-induced CPA are in quite large ranges. Interestingly, the longitudinal polarization fraction of $B_s \rightarrow K^{*-}K^{*+}$ could be suppressed as low as 0.30. Therefore future experimental measurements of these decays could shrink or reveal the relevant NP parameter spaces. It is found that the squark exchange coupling $\lambda''_{132}\lambda''_{112}$ could have large contributions to the branching ratios of $B_s \rightarrow K^{*-}\pi^+$, $K^-\rho^+$, and enhance the longitudinal direct CP asymmetry of $B_s \rightarrow K^{*-}\rho^+$ to $\sim 70\%$. The longitudinal polarization fraction of $B_s \rightarrow K^{*-}\rho^+$ could be suppressed too. The slepton exchange coupling $\lambda'_{i13}\lambda'_{i11}$ could enhance the branching ratio of $B_s \rightarrow K^{*-}\pi^+$ by few times. We also have presented correlations between these physical observable quantities and the constrained parameter spaces of RPV couplings in Figs. 3-6. The results in this paper could be useful for probing RPV SUSY effects and searching direct RPV signals at Tevatron and LHC in the near future.

Acknowledgments

The work is supported by National Science Foundation under contract Nos.10675039 and 10735080. The work of Ru-Min Wang was supported by Brain Korea 21 Project.

References

- [1] A. Abulencia *et al.* [CDF Collaboration], Phys. Rev. Lett. **97**, 211802 (2006) [arXiv:hep-ex/0607021].
- [2] M. Morello [CDF Collaboration], Nucl. Phys. Proc. Suppl. **170**, 39 (2007) [arXiv:hep-ex/0612018].

- [3] M. Morello [CDF Collaboration], arXiv:0810.3258 [hep-ex].
- [4] T. Altonen *et al.* [CDF Collaboration], arXiv:0812.4271 [hep-ex].
- [5] [CDF Collaboration], “Measurement of branching fractions and direct CP asymmetries of $B_{(s)}^0 \rightarrow h^+ h'^-$ decays in 1fb^{-1} ,” and the updated results on April 10, 2008 may be found on <http://www-cdf.fnal.gov/physics/new/bottom/bottom.html> [Note 8579v1].
- [6] M. Beneke and M. Neubert, Nucl. Phys. B **675**, 333 (2003) [arXiv:hep-ph/0308039].
- [7] A. Ali *et al.*, Phys. Rev. D **76**, 074018 (2007) [arXiv:hep-ph/0703162].
- [8] A. R. Williamson and J. Zupan, Phys. Rev. D **74**, 014003 (2006) [Erratum-ibid. D **74**, 03901 (2006)] [arXiv:hep-ph/0601214].
- [9] M. Beneke, G. Buchalla, M. Neubert and C. T. Sachrajda, Phys. Rev. Lett. **83**, 1914 (1999) [arXiv:hep-ph/9905312]; Nucl. Phys. B **591**, 313 (2000) [arXiv:hep-ph/0006124]; Nucl. Phys. B **606**, 245 (2001) [arXiv:hep-ph/0104110].
- [10] Y. Y. Keum, H. n. Li and A. I. Sanda, Phys. Lett. B **504**, 6 (2001) [arXiv:hep-ph/0004004]; Phys. Rev. D **63**, 054008 (2001) [arXiv:hep-ph/0004173]; Y. Y. Keum and H. n. Li, Phys. Rev. D **63**, 074006 (2001) [arXiv:hep-ph/0006001]; C. D. Lü, K. Ukai and M. Z. Yang, Phys. Rev. D **63**, 074009 (2001) [arXiv:hep-ph/0004213]; Y. Y. Keum and A. I. Sanda, Phys. Rev. D **67**, 054009 (2003) [arXiv:hep-ph/0209014].
- [11] C. W. Bauer, S. Fleming and M. E. Luke, Phys. Rev. D **63**, 014006 (2000) [arXiv:hep-ph/0005275]; C. W. Bauer, S. Fleming, D. Pirjol and I. W. Stewart, Phys. Rev. D **63**, 114020 (2001) [arXiv:hep-ph/0011336]; C. W. Bauer and I. W. Stewart, Phys. Lett. B **516**, 134 (2001) [arXiv:hep-ph/0107001].
- [12] S. Baek, D. London, J. Matias and J. Virto, JHEP **0612**, 019 (2006) [arXiv:hep-ph/0610109].
- [13] M. Beneke, J. Rohrer and D. Yang, Nucl. Phys. B **774**, 64 (2007) [arXiv:hep-ph/0612290].
- [14] C. H. Chen, Phys. Lett. B **520**, 33 (2001) [arXiv:hep-ph/0107189].

- [15] X. Q. Li, G. R. Lu and Y. D. Yang, Phys. Rev. D **68**, 114015 (2003) [Erratum-ibid. D **71**, 019902 (2005)] [arXiv:hep-ph/0309136].
- [16] S. W. Lin *et al.* [Belle Collaboration], Nature **452**, 332 (2008).
- [17] B. Aubert *et al.* [BABAR Collaboration], Phys. Rev. Lett. **99**, 021603 (2007) [arXiv:hep-ex/0703016].
- [18] K. Abe *et al.* [Belle Collaboration], Phys. Rev. Lett. **93**, 021601 (2004) [arXiv:hep-ex/0401029].
- [19] B. Aubert *et al.* [BABAR Collaboration], Phys. Rev. Lett. **95**, 151803 (2005) [arXiv:hep-ex/0501071].
- [20] B. Aubert *et al.* [BABAR Collaboration], arXiv:0807.4226 [hep-ex].
- [21] B. Aubert [BABAR Collaboration], [arXiv:hep-ex/0408093];
- [22] J. Zhang *et al.* [BELLE Collaboration], [arXiv:hep-ex/0505039].
- [23] B. Aubert *et al.* [BABAR Collaboration], Phys. Rev. Lett. **98**, 051801 (2007) [arXiv:hep-ex/0610073].
- [24] S. Baek, JHEP **0607**, 025 (2006) [arXiv:hep-ph/0605094];
- [25] Y. L. Wu, Y. F. Zhou and C. Zhuang, Phys. Rev. D **74**, 094007 (2006) [arXiv:hep-ph/0609006].
- [26] C. Dariescu, M. A. Dariescu, N. G. Deshpande and D. K. Ghosh, Phys. Rev. D **69**, 112003 (2004) [arXiv:hep-ph/0308305].
- [27] Q. Chang, X. Q. Li and Y. D. Yang, JHEP **0809**, 038 (2008) [arXiv:0807.4295 [hep-ph]];
Q. Chang, X. Q. Li and Y. D. Yang, JHEP **0706**, 038 (2007) [arXiv:hep-ph/0610280].
- [28] A. J. Buras, R. Fleischer, S. Recksiegel and F. Schwab, Acta Phys. Polon. B **36**, 2015 (2005) [arXiv:hep-ph/0410407].
- [29] Y. D. Yang, R. Wang and G. R. Lu, Phys. Rev. D **73**, 015003 (2006) [arXiv:hep-ph/0509273].

- [30] D. London, J. Matias and J. Virto, Phys. Rev. D **71**, 014024 (2005) [arXiv:hep-ph/0410011].
- [31] S. Baek, D. London, J. Matias and J. Virto, JHEP **0602**, 027 (2006) [arXiv:hep-ph/0511295]; S. Descotes-Genon, J. Matias, J. Virto, Phys. Rev. Lett. **97**, 061801(2006)[arXiv:hep-ph/0603239].
- [32] R. Fleischer and M. Gronau, Phys. Lett. B **660**, 212 (2008) [arXiv:0709.4013 [hep-ph]].
- [33] S. Weinberg, Phys. Rev. D **26**, 287 (1982).
- [34] N. Sakai and T. Yanagida, Nucl. Phys. B **197**, 533 (1982); C. S. Aulakh and R. N. Mohapatra, Phys. Lett. B **119**, 136 (1982).
- [35] R. Barbier *et al.*, Phys. Rept. **420**, 1 (2005) [arXiv:hep-ph/0406039], and references therein.
- [36] R. Barbier *et al.*, [arXiv:hep-ph/9810232].
- [37] M. Chemtob, Prog. Part. Nucl. Phys. **54**, 71 (2005) [arXiv:hep-ph/0406029].
- [38] B. Allanach *et al.* [R parity Working Group Collaboration], [arXiv:hep-ph/9906224], and references therein.
- [39] G. Buchalla, A. J. Buras and M. E. Lautenbacher, Rev. Mod. Phys. **68**, 1125 (1996) [arXiv:hep-ph/9512380].
- [40] G. Bhattacharyya, A. Datta and A. Kundu, J. Phys. G **30**, 1947 (2004) [arXiv:hep-ph/0212059].
- [41] M. Gronau, Phys. Lett. B **233**, 479 (1989).
- [42] J. Soto, Nucl. Phys. B **316**, 141 (1989).
- [43] A. Ali, G. Kramer and C. D. Lu, Phys. Rev. D **59**, 014005 (1999) [arXiv:hep-ph/9805403].
- [44] W. F. Palmer and Y. L. Wu, Phys. Lett. B **350**, 245 (1995) [arXiv:hep-ph/9501295].
- [45] R. Fleischer, J. Phys. G **32**, R71 (2006) [arXiv:hep-ph/0512253].

- [46] W. M. Yao *et al.* [Particle Data Group], J. Phys. G **33**, 1 (2006) and 2007 partial update for edition 2008.
- [47] J. Charles et al. (CKMfitter Group), Eur. Phys. J. C **41**, 1 (2005) [hep-ph/0406184], updated results and plots available at: <http://ckmfitter.in2p3.fr/>.
- [48] P. Ball and R. Zwicky, Phys. Rev. D **71**, 014015 (2005) [arXiv:hep-ph/0406232]; Phys. Rev. D **71**, 014029 (2005) [arXiv:hep-ph/0412079].
- [49] G. Duplancic, and B. Melic, Phys. Rev. D **78**, 054015 (2008) [arXiv:0805.4170].
- [50] V. Lubicz and C. Tarantino, [arXiv:0807.4605 [hep-lat]].
- [51] V. M. Braun, D. Y. Ivanov and G. P. Korchemsky, Phys. Rev. D **69**, 034014 (2004) [arXiv:hep-ph/0309330].
- [52] D. K. Ghosh, X. G. He, B. H. J. McKellar and J. Q. Shi, JHEP **0207**, 067 (2002) [arXiv:hep-ph/0111106].